Supporting Information

Modified Reaction Kinetics in Ester-based Electrolyte to Boost Sodium Storage Performance: A Case Study of $MoS_2/Ti_3C_2T_x$ Hybrid

Jiabao Li*[a], Shaocong Tang[a], Ziqian Li[a], Jingjing Hao[a], Tianyi Wang[a], Likun Pan*[b], Chengyin Wang*[a]

[a]School of Chemistry and Chemical Engineering, Yangzhou University, 180 Si-Wang-Ting Road, Yangzhou, Jiangsu 225002, China

[b]Shanghai key laboratory of Magnetic Resonance, School of Physics and Electronic Science, East China Normal University, Shanghai 200241, China

Corresponding Authors: jiabaoli@yzu.edu.cn (Jiabao Li); lkpan@phy.ecnu.edu.cn (Likun Pan); wangcy@yzu.edu.cn (Chengyin Wang)

Material Characterization

Generally, the morphology investigation for as-prepared samples was conducted through filed-emission scanning electron microscopy (Zeiss_Supra55) and transmission electron microscopy (Tecnai 12). The X-ray diffraction patterns were collected by the D8 ADVANCE using Cu Kα radiation source (λ = 1.54056 Å). The X-ray photoelectron spectroscopy measurements were conducted on an electron spectrometer (ESCALAB 250Xi) to detect the chemical component of as-prepared sample and the solid electrolyte interface.

Electrochemical Measurement

For the fabrication of working electrode, desired MoS2/Ti3C2Tx, conductive agent (Super P), and binder (carboxymethyl cellulose) with a mass ratio of 8:1:1 was dispersed into deionized water and further ground to from a uniform slurry, which was then coated on a clean copper foil and vacuum dried at 100 °C overnight. In regard to the cell assembly, sodium foil and Whatman glass fiber were employed as the counter electrode and separator, separately. To investigate the effect of electrolytes on the electrochemical performance, 1.0 M NaPF6 in diethylene glycol dimethyl ether (DEGDME) and 1.0 M NaPF6 in ethylene carbonate/diethyl carbonate (EC/DEC) were employed. The electrochemical tests were conduced on the LAND 2001A battery test system, and the cyclic voltammetry measurements were conducted on an electrochemical workstation (CHI 660B), and the electrochemical impedance spectra were also collected from the same workstation from 0.1 Hz to 1000 kHz.

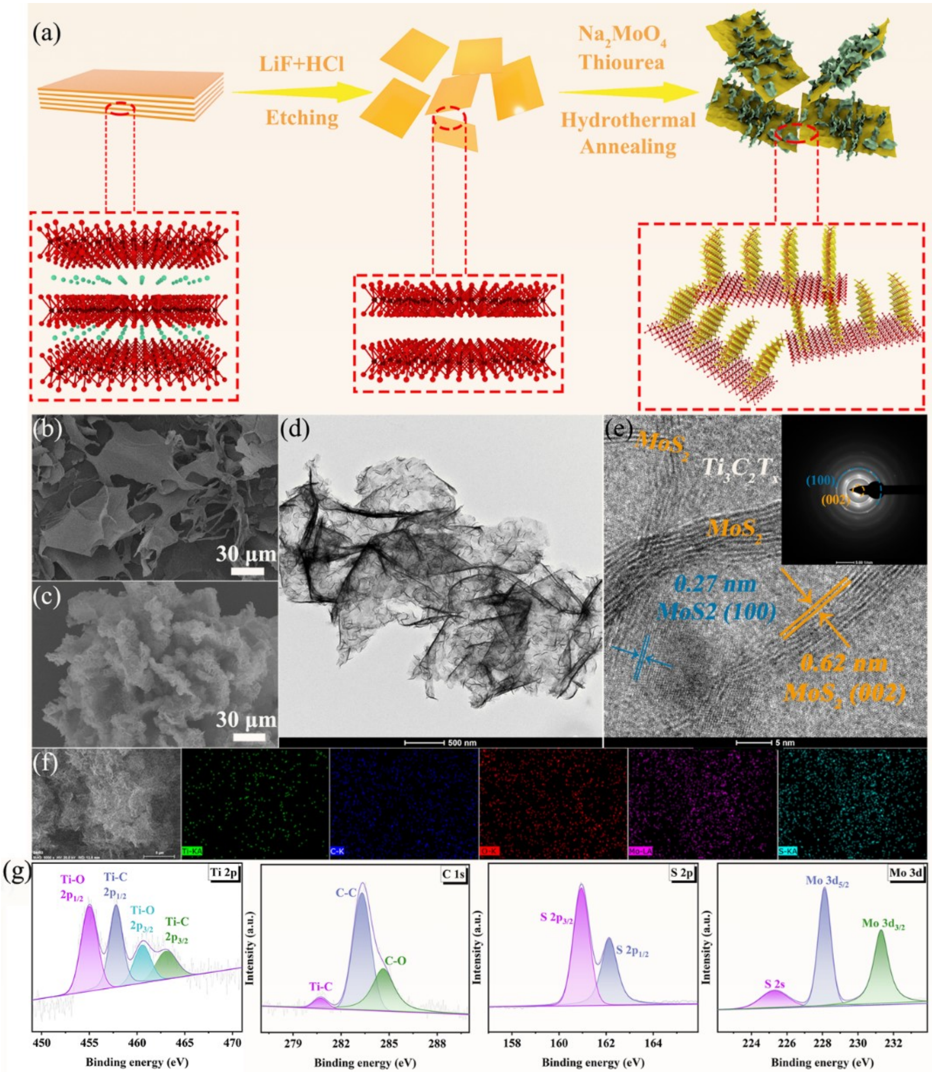

Fig. S1 Schematic presentation of the process for the synthesis of target $MoS_2/Ti_3C_2T_x$ (a). FESEM images of $Ti_3C_2T_x$ MXene (b) and $MoS_2/Ti_3C_2T_x$ (c). TEM image (d), HRTEM image (e, the inset is the SAED pattern), and elemental mapping (f) of $MoS_2/Ti_3C_2T_x$. XPS spectra (g) of $MoS_2/Ti_3C_2T_x$: Ti 2p, C 1s, S 2p, Mo 3d.

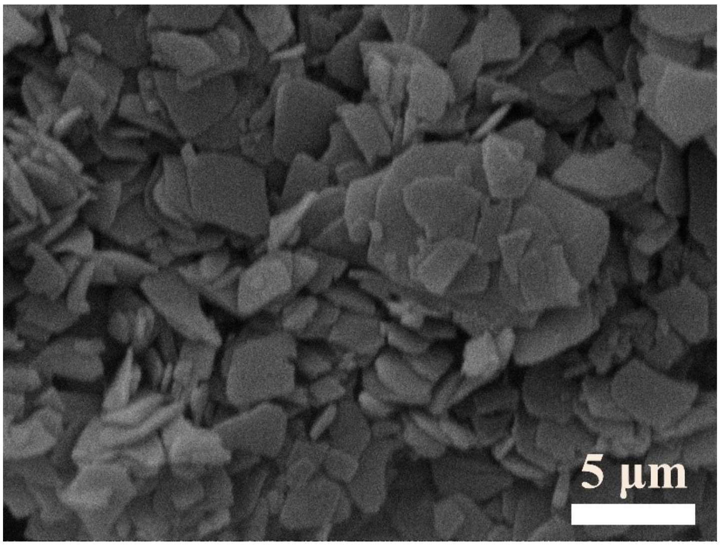

Fig. S2 FESEM image of Ti_3AlC_2.

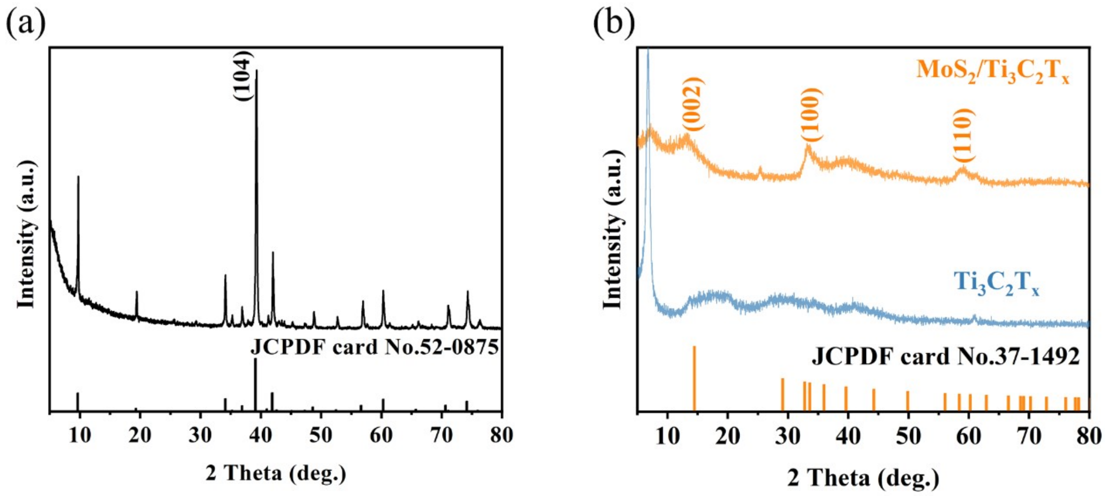

Fig. S3 XRD patterns of Ti_3AlC_2 (a), $Ti_3C_2T_x$ and $MoS_2/Ti_3C_2T_x$ (b).

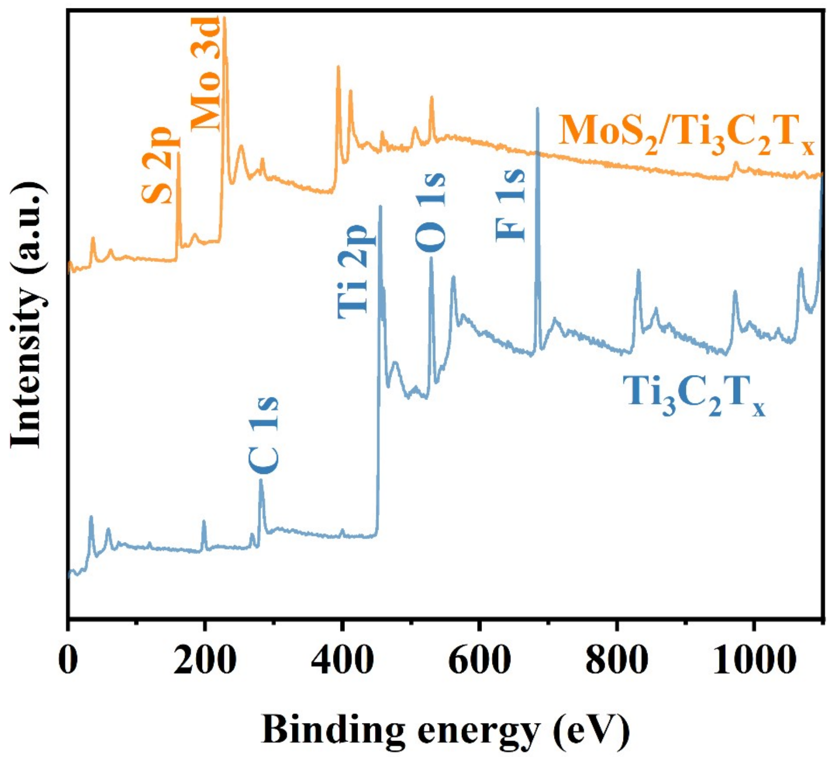

Fig. S4 XPS survey spectra of $Ti_3C_2T_x$ and $MoS_2/Ti_3C_2T_x$.

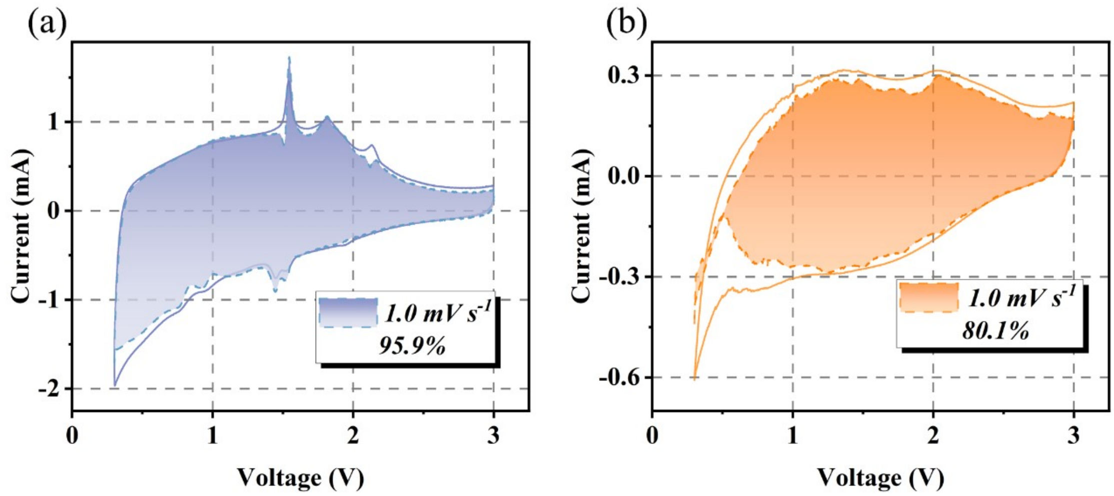

Fig. S5 Capacitive contribution to charge storage of $MoS_2/Ti_3C_2T_x$ at 1.0 mV s^{-1} in DEGDME (a) and EC/DEC (b) electrolytes.

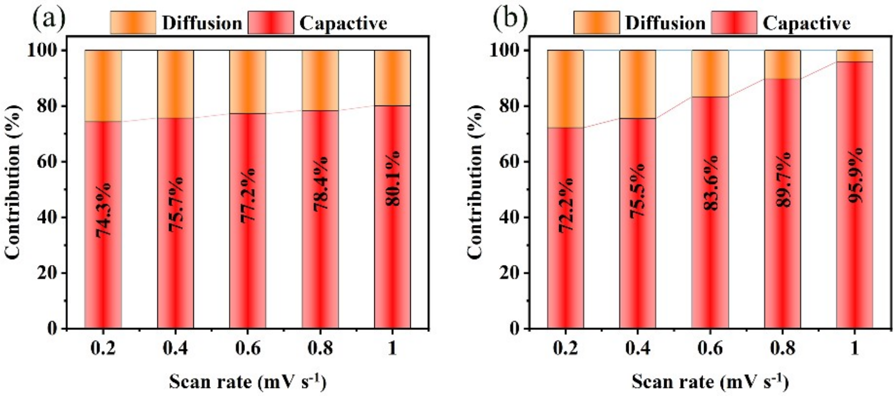

Fig. S6 The separated contributions to charge storage from diffusion and pseudocapacitive effect of the target $MoS_2/Ti_3C_2T_x$ electrode in EC/DEC (a) and DEGDME (b) electrolyte.

In principle, according to Fick's second law of diffusion, the diffusion coefficient of Na^+ in target electrode can be calculated by Equation 4:

$$D_{Na^+} = \frac{4}{\pi\tau}\left(\frac{m_b V_m}{M_b S}\right)^2\left(\frac{\Delta E_S}{\Delta E_t}\right)^2, \tau \ll L^2 / D_{Na^+} \quad (4)$$

where τ represents the time of applied current, and ΔE_s and ΔE_τ represent the change of steady-state voltage after a discharge pulse and the change of voltage during the discharge pulse, respectively. As for the V_m, M_b, mb, and S, they correspond to the molar volume, molecular weight, and mass loading of active material in the electrode and the surface area of electrode, respectively.

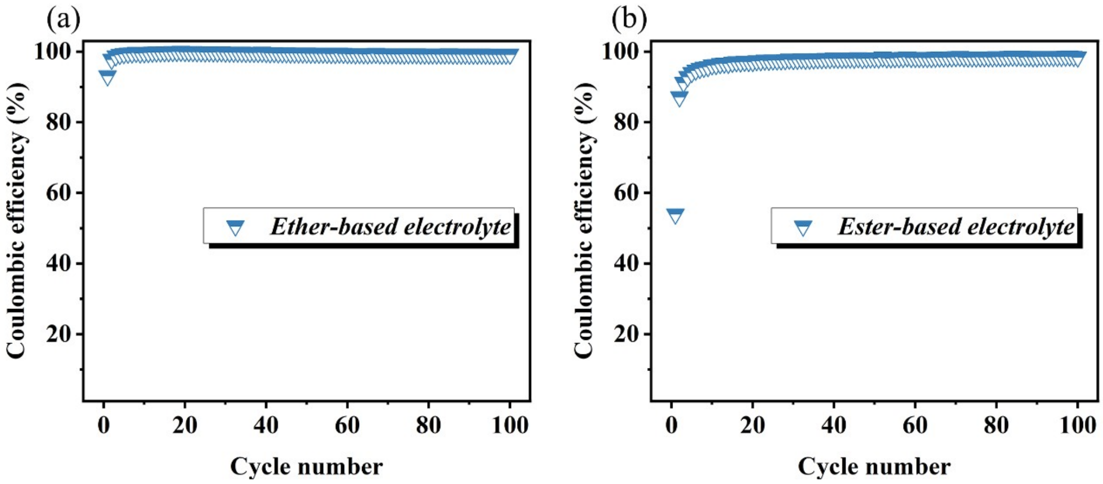

Fig. S7 The Coulombic efficiency of $MoS_2/Ti_3C_2T_x$ in DEGDME (a) and EC/DEC (b) electrolytes at 0.1 A g^{-1}.

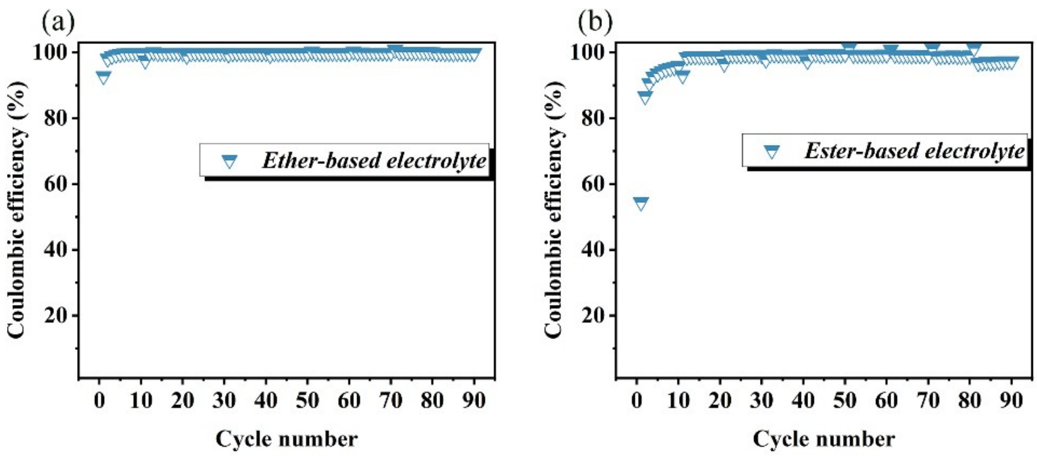

Fig. S8 The Coulombic efficiencies of $MoS_2/Ti_3C_2T_x$ upon rate tests in DEGDME (a) and EC/DEC (b) electrolyte.

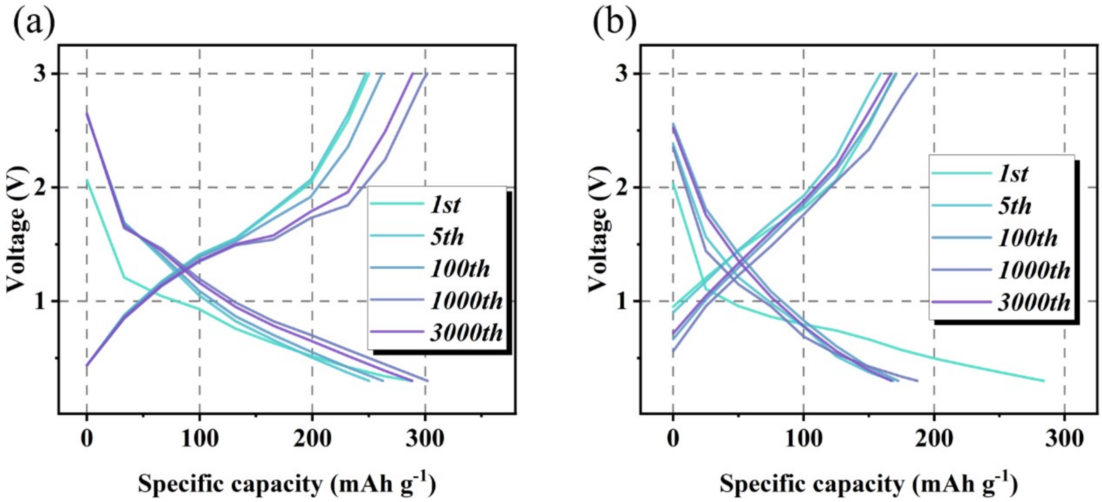

Fig. S9 Discharge/charge profiles of $MoS_2/Ti_3C_2T_x$ at 3.0 A g^{-1} in DEGDME (a) and EC/DEC (b) electrolytes.

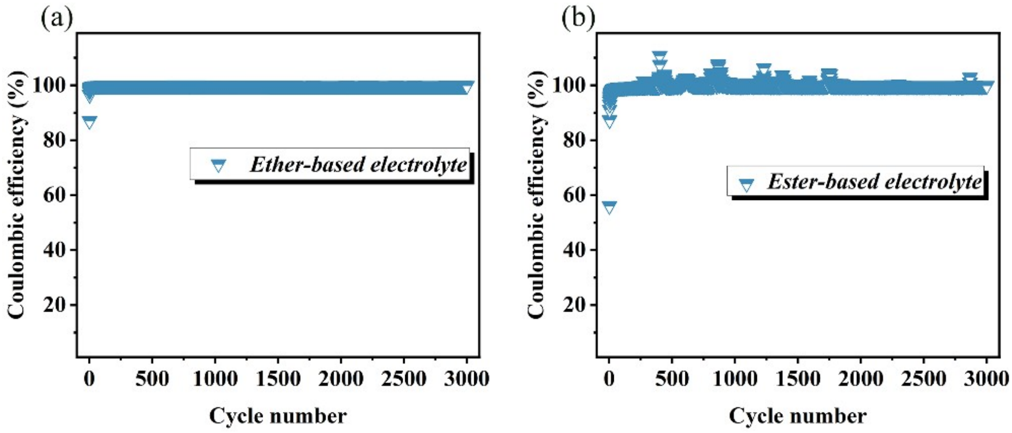

Fig. S10 The Coulombic efficiencies of $MoS_2/Ti_3C_2T_x$ upon the long-term cycling at 3.0 A g^{-1} in DEGDME (a) and EC/DEC (b) electrolyte.

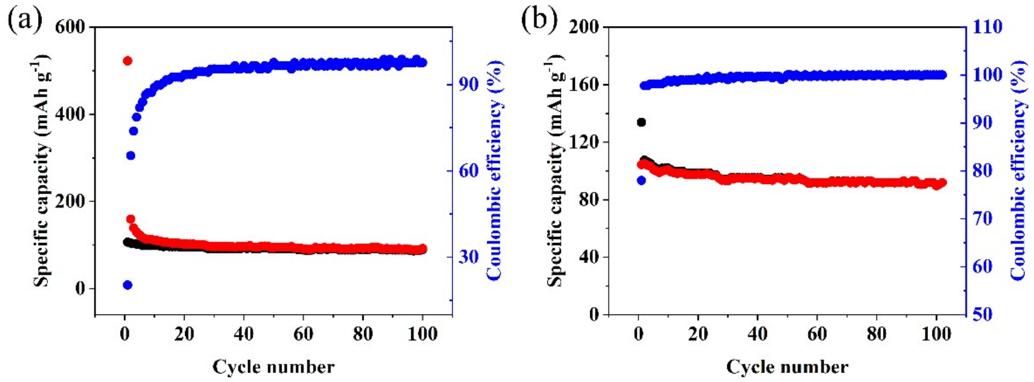

Fig. S11 The cycling performance of $Ti_3C_2T_x$ MXene in EC/DEC and DEGDME electrolyte at 0.2 A g^{-1}.

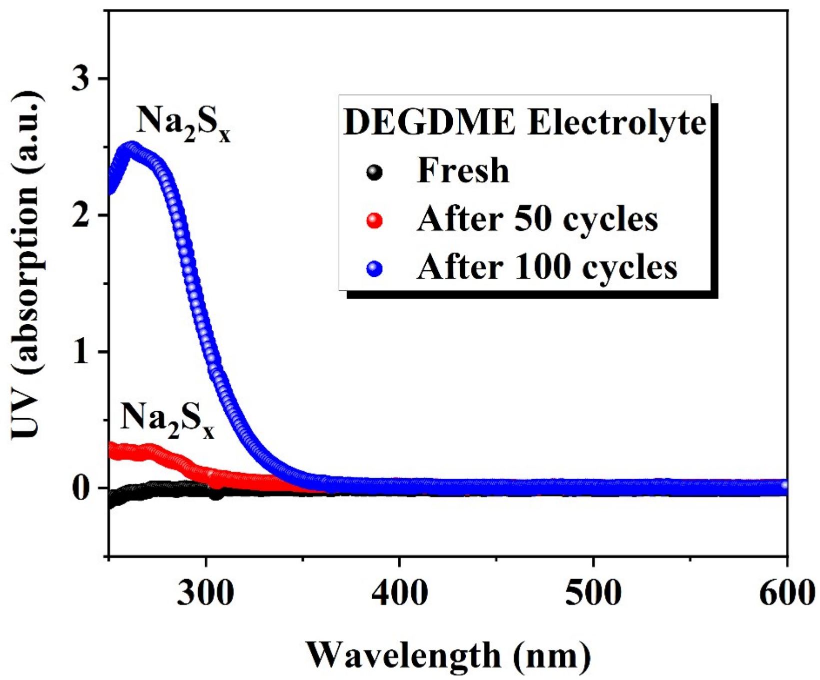

Fig. S12 UV-vis spectra of DEGDME after the immersion (overnight) of cycled separator in DEGDME electrolyte.

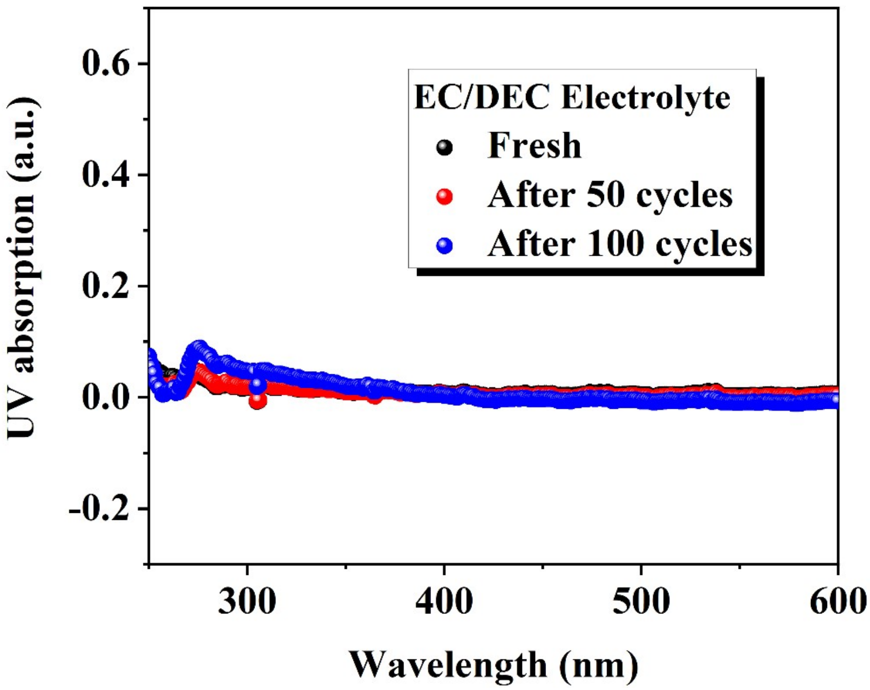

Fig. S13 Fig. S8 UV-vis spectra of EC/DEC after the immersion (overnight) of cycled separator in EC/DEC electrolyte.

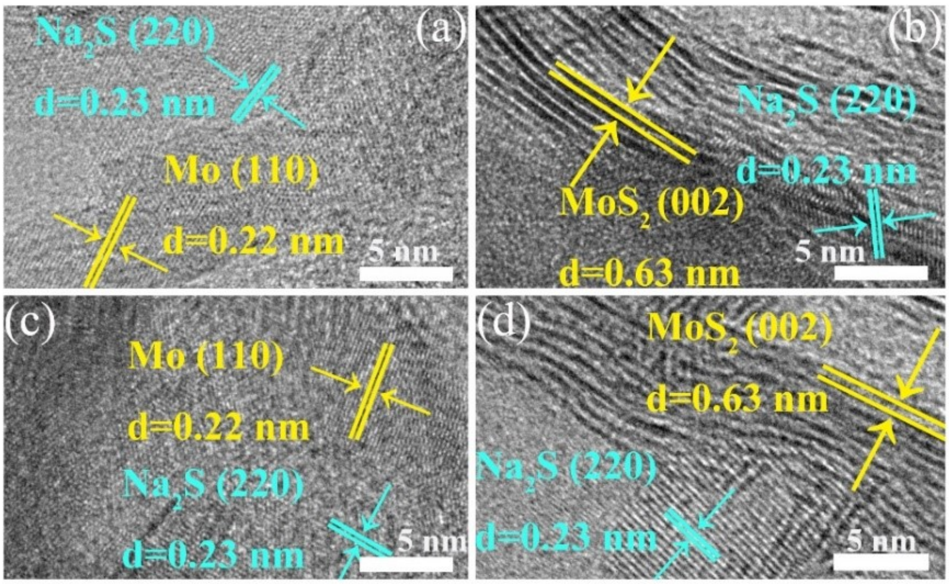

Fig. S14 The HRTEM images of $MoS_2/Ti_3C_2T_x$ at the discharged and charged states in DEGDME (a and b) and EC/DEC (c and d) electrolyte.

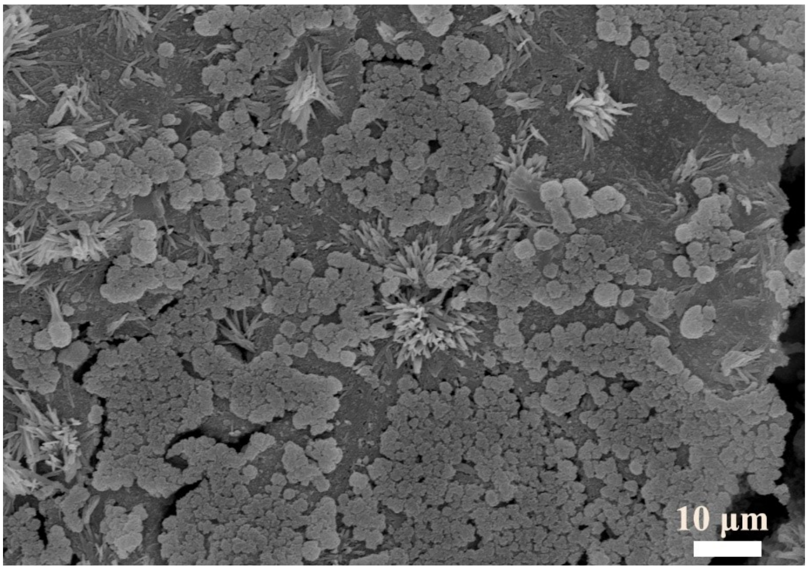

Fig. S15 SEM images of the $MoS_2/Ti_3C_2T_x$ electrode after 100 cycles at 3.0 A g^{-1} in EC/DEC electrolyte.

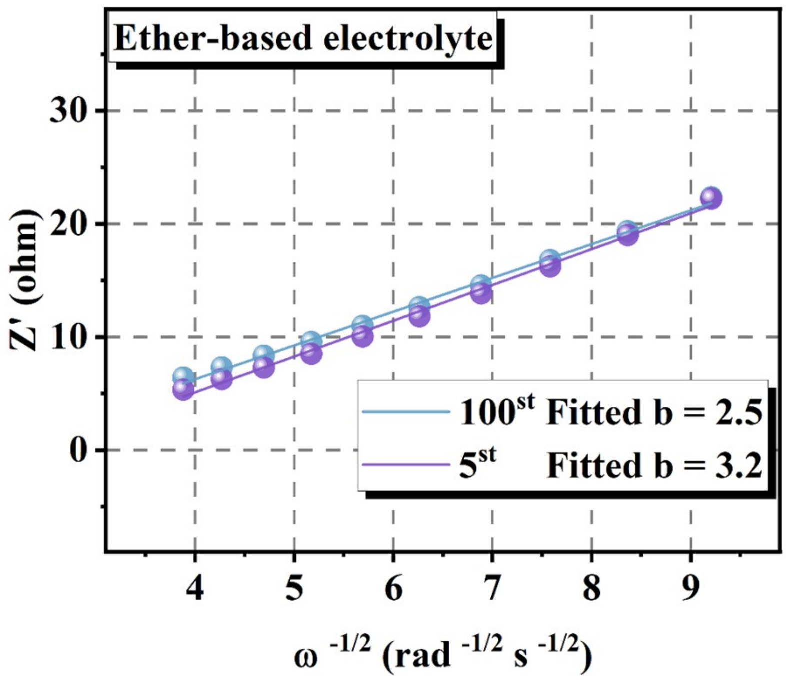

Fig. S16 Fitted lines of Z′ versus $\omega^{-1/2}$ plots before and after 100 cycles for the $MoS_2/Ti_3C_2T_x$ electrode in DEGDME electrolyte.

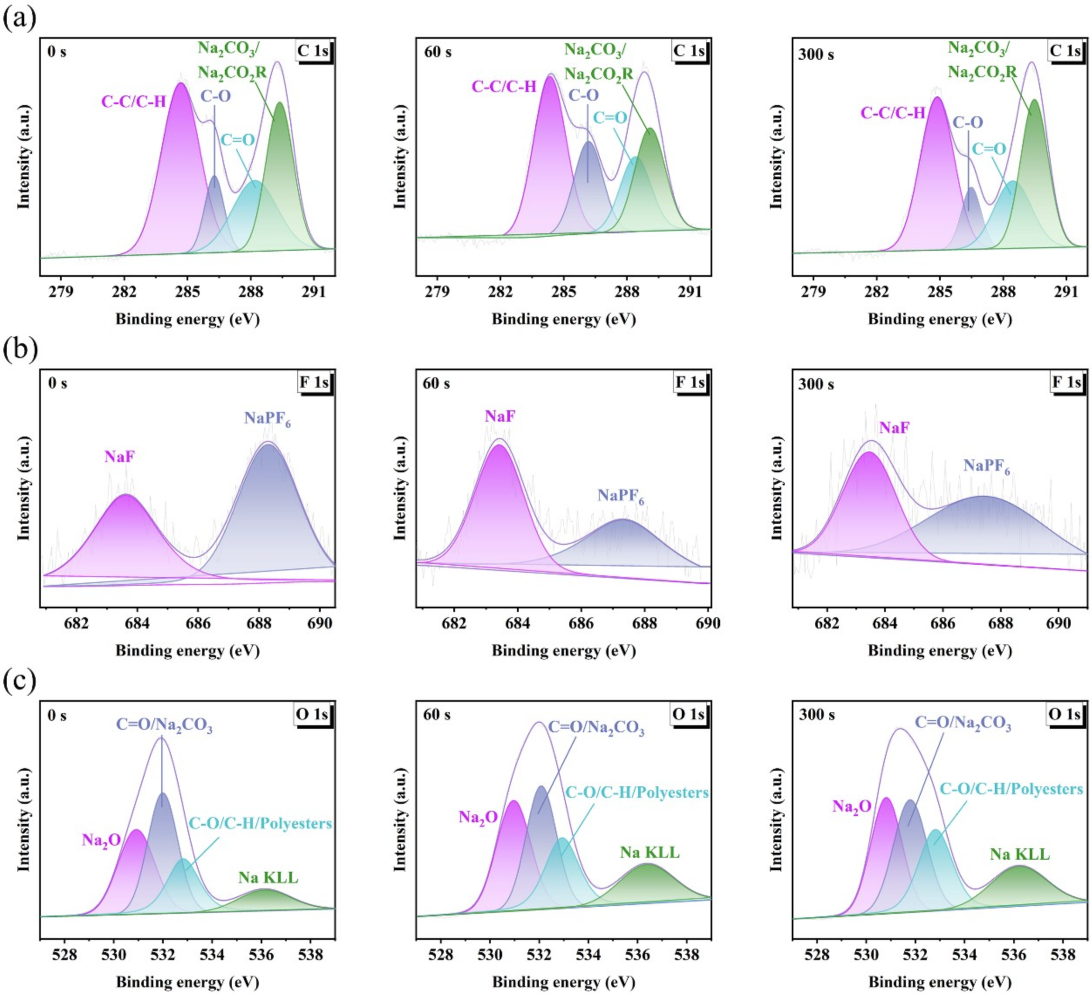

Fig. S17 XPS spectra as a function of SEI depth for $MoS_2/Ti_3C_2T_x$ after 5 cycles at 0.1 A g^{-1} in EC/DEC electrolytes: C 1s (a), O 1s (b), and F 1s (c).